II International Conference on Particle-based Methods – Fundamentals and Applications
PARTICLES 2011
E. Oñate and D.R.J. Owen (Eds)

HUMAN BODAY DAMAGE ANALYSIS BY SPH METHOD

XUELONG LU*, HIROMASA KITAKAWA† TAKUYA MUKAI*YUZURU SAKAI*,

* Yokohama National University 79-1 Tokiwadai,Hodogaya-ku,Yokohama 240-8501 Japan
e-mail: lu-xuelong-xg@ynu.jp
* Yokohama National University 79-1 Tokiwadai,Hodogaya-ku,Yokohama 240-8501 Japan
e-mail: ysakai@ynu.ac.jp
* Yokohama National University 79-1 Tokiwadai,Hodogaya-ku,Yokohama 240-8501 Japan
e-mail: s-fleet@cd6.so-net.ne.jp
† So-net Enterinment Coorporation 2-1-1 Osaki,Shinagawa-ku,Tokyo 141-6010 Japan

Key words: SPH, Particle Method,GPU volume rendering, CT image, Impact Problems.

Abstract. In order to evaluate the biological properties of a human head response at impacts accidents, authors have been developing the SPH (Smooth Particle Hydrodynamics) particle model of the whole human head and analyzing dynamically in simulating high velocity impact accident. In this report, authors have shown how to make a particle model of a head from real CT scan images directly and how to render the model in computer graphics using GPU and the algorithm for elastic-plastic analysis of a head model. The results from the simulations could explain one of injury mechanisms of a human head in actual car accidents.

1 INTRODUCTION

SPH (Smoothed Particle Hydrodynamics)[1-7] is a gridless Lagrangian technique which is promising as a possible alternative to numerical techniques currently used to analyze high deformation impulsive loading events, such as hypervelocity impact or explosive loading of materials, elastic-plastic analysis[8], heat transfer analysis[9] and other various phenomenon, While Eulerian techniques are appropriate to handle the gross motions associated with the large deformations , however detailed analysis is difficult because of the lack of history at the arbitral positions of the body by using Eulerian grid. Standard Lagrangian techniques are convenient to keep accurate histories of the events associated with each Lagrangian particles.

In general material models which describe the behavior of matter under extreme loading conditions usually require keeping precise histories at each material element or point. While it is relatively simple to produce this information from Lagrangian code calculations, it is a much more difficult task for an Eulerian code while Lagrangian techniques are excellent at tracking the history associated with each material point and can easily save the required information.

The basic SPH technique was first introduced by Lucy [1] and Gingold and Monahan [2] in 1977, and two comprehensive reviews are presented by Benz [3] and Monaghan [4]. More recently, the effect of strength was added by Libersky and Petschek [5], axisymmetric algorithms were developed by Johnson et al. [6], and Petschek and libersky[7].

In recent years, researchers have also shown the values of particle method for medical and biological analysis Because the human body has complex geometries, it is very difficult to analyze by using mesh type models. Authors have confirmed the utility of a particle method for analyzing the structural problems of the human body . This study has been aimed to reproduce a human head particle model by using medical information (CT scanning data) and simulate the impact accident of a human head against a wall under high velocity (50m/s).

2 ANALYSIS METHOD

2.1.1 Theory of SPH

The foundation of SPH is one of the interpolation techniques. The equation of motion and the conservation laws of substance, in the form of partial differential equations, are introduced into integral equations through the use of an interpolation function (weight function) that gives the estimate of the field variables at a point. In numerical process, information is given at discrete points, so that the integrals are evaluated as summing over neighboring particles. Figure.1 shows the concept of SPH method. Consider a function f and a kernel w which has a radius (support domain) h , the kernel estimate is

$$f(x) \approx \int f(x')w(x-x',h)dx' \tag{1}$$

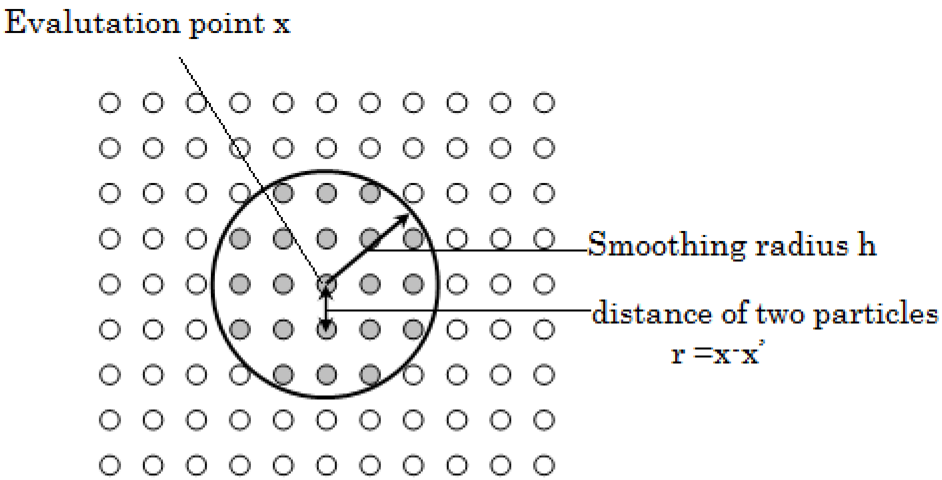

Figure1 The concept of SPH

As a typical weight function we employed the spline function of 3 degrees which is usually used in SPH analysis [10]. The approximation for spatial derivatives is obtained by substituting $\nabla \bullet f(x)$ for $f(x)$ in Eq. (1)

$$\nabla \bullet f(x) \approx \int \nabla \bullet f(x')W(x-x',h)dx' \tag{2}$$

In general physical parameters $f(x)$ in a continuum is interpolated using a weight function and the discrete kernel estimate and its spatial derivative become

$$f(x) \approx \sum_{J=1}^{N} \frac{m^J}{\rho^J} f(x^J) W(x - x^J, h) \tag{3}$$

And

$$\nabla \bullet f(x) \approx -\sum_{J=1}^{N} \frac{m^J}{\rho^J} f(x^J) \bullet \nabla W(x - x^J, h) \tag{4}$$

Where m is the mass, ρ is the density of the material and J is the interpolation points within a support domain. In this study, the elastic-plastic analysis is applied to human head impact against a rigid wall. The acceleration of a particle can be represented as follows using the stress divergence.

$$a = \frac{1}{\rho} \nabla \cdot \sigma \tag{5}$$

Where σ is Cauchy stress tensor and a is acceleration . The acceleration of particle i is obtained as

$$a_i^I = -\sum_{J=1}^{N} m^J \sum_{j=1}^{3} \frac{\sigma_{ij}^J}{\rho^I \rho^J} \frac{\partial W}{\partial x_j^J} \tag{6}$$

The variations of the Eq. (6) are sometime used. By using the stress tensor at point I, the Eq. (6) becomes

$$a_i^I = -\sum_{J=1}^{N} m^J \sum_{j=1}^{3} \left[\left(\frac{\sigma_{ij}}{\rho^2} \right)^I + \left(\frac{\sigma_{ij}}{\rho^2} \right)^J \right] \frac{\partial W}{\partial x_j^J} \tag{7}$$

As the above equation, acceleration of any point in a stress field will be obtained. The interaction between Particle I and particle J is equal. That is, the law of conservation of momentum is guaranteed exactly.

Velocity gradient is given using Eq. (4)

$$\left(\frac{\partial V_i}{\partial x_j} \right)^I = -\sum_{J=1}^{N} \frac{m^J}{\rho^I} V_i^J \frac{\partial W}{\partial x_j^J} \tag{8}$$

And

$$\left(\frac{\partial V_i}{\partial x_j} \right)^I = \frac{1}{\rho^I} \sum_{J=1}^{N} m^J (V_i^I - V_j^J) \frac{\partial W}{\partial x_j^J} \tag{9}$$

The latter relation has the advantage that the contribution to the strain rate tensor from particles I and J is zero if their relative velocity is zero. As Eq. (9), using the known particle positions and stress to seek acceleration at time t^n .velocity and position is as follow.

$$V_i^{I,n+\frac{1}{2}} = V_i^{I,n-\frac{1}{2}} + \frac{1}{2} \left(\Delta t^{n+\frac{1}{2}} + \Delta t^{n-\frac{1}{2}} \right) a_i^{I,n} \tag{10}$$

$$x_i^{I,n+1} = x_i^{I,n} + \Delta t^{n+\frac{1}{2}} V_i^{I,n+\frac{1}{2}} \tag{11}$$

Particle density at time t^{n+1} is

$$\rho(x) = \sum_{J=1}^{N} m^J W(x - x^J, h) \tag{12}$$

Strain rate tensor is obtained by velocity gradient as follow equation.

$$\dot{\varepsilon}_{ij} = \frac{1}{2}\left(\frac{\partial V_i}{\partial x_j} + \frac{\partial V_j}{\partial x_i}\right). \tag{13}$$

Vorticity tensor is obtained as

$$\omega_{ij} = \frac{1}{2}\left(\frac{\partial V_i}{\partial x_j} - \frac{\partial V_j}{\partial x_i}\right) \tag{14}$$

2.1.2 Artificial viscosity

In SPH analysis the discretization equation has inevitably numerical instability. To control the numerical instability, artificial viscosity terms are generally used. Just like the finite difference method, the artificial viscous stresses are given as follow equation.

$$Q = \rho b_1^2 \left(\frac{\dot{\rho}}{\rho}\right)^2 + \rho b_2 C\left(\frac{\dot{\rho}}{\rho}\right) \tag{15}$$

Where b_1 and b_2 are length constant. c is the sound speed. The artificial viscous stress is

$$Q = \rho B_1^2 l^2 \left(\frac{\dot{\rho}}{\rho}\right)^2 + \rho B_2 l C\left(\frac{\dot{\rho}}{\rho}\right) \tag{16}$$

Hence, equation of motion that containing artificial viscosity is

$$a_i^I = -\sum_{J=1}^{N} m^J \sum_{j=1}^{3} \left[\left(\frac{\sigma_{ij} - Q\delta_{ij}}{\rho^2}\right)^I + \left(\frac{\sigma_{ij} - Q\delta_{ij}}{\rho^2}\right)^J\right] \frac{\partial W}{\partial x_j^J} \tag{17}$$

As Monaghan pointed out follow equation, a common technique used is

$$Q^{IJ} = \rho^2 \Pi^{IJ} \tag{18}$$

Where

$$\Pi^{IJ} = \frac{\alpha C^{IJ} \mu^{IJ} - \beta(\mu^{IJ})^2}{\rho^{IJ}} \tag{19}$$

$$\mu^{IJ} = \frac{h\sum_{j=1}^{3}\left(V_j^I - V_j^J\right)\left(x_j^I - x_j^J\right)}{\left(\left|x_j^I - x_j^J\right|\right)^2 + \varepsilon h^2} \tag{20}$$

$$C^{IJ} = \frac{1}{2}\left(C^I + C^J\right) \tag{21}$$

$$\rho^{IJ} = \frac{1}{2}\left(\rho^I + \rho^J\right) \tag{22}$$

Thus,

$$a_i^I = -\sum_{J=1}^{N} m^J \sum_{j=1}^{3}\left[\left(\frac{\sigma_{ij}}{\rho^2}\right)^I + \left(\frac{\sigma_{ij}}{\rho^2}\right)^J + \Pi^{IJ}\delta_{ij}\right]\frac{\partial W}{\partial x_j^J} \tag{23}$$

By using the above equation we can solve the impact analysis without the particle turbulent oscillations from the numerical instability.

2.1.3 Elastic plastic analysis

SPH algorithm for elastic-plastic analysis method has been developed by authors. In the case that strain rate effects are not into account by using the elastic plastic algorithm in finite element analysis. In the finite element method, the yield judgment is performed at the numerical integration points of the element or the center point of element, while in SPH method yield condition is performed for each particle of the model.

SPH method used the yield condition which be applied in the finite element method. A typical expression of the Mises yield condition is the yield stress of material.

In this analysis we have used the Elastic-plastic problems always use deformation theory and incremental theory. SPH method interpolates explicitly, that easy to handle the incremental amount of physical expression. So authors use the incremental theory in elastic-plastic analysis too. In the elastic region

$$\{d\varepsilon\} = \begin{Bmatrix} d\sigma_x \\ d\sigma_y \\ d\tau_{xy} \end{Bmatrix} = \frac{E}{1-v^2}\begin{bmatrix} 1 & v & 0 \\ v & 1 & 0 \\ 0 & 0 & \dfrac{1-v}{2} \end{bmatrix}\begin{Bmatrix} d\varepsilon_x \\ d\varepsilon_y \\ d\gamma_{xy} \end{Bmatrix} = \left[D_e\right]\{d\varepsilon\} \tag{24}$$

In the plastic region

$$\{d\sigma\} = \begin{bmatrix} \dfrac{E}{1-v^2} - \dfrac{S_1^2}{S} & \dfrac{vE}{1-v^2} - \dfrac{S_1S_2}{S} & -\dfrac{S_1S_6}{S} \\ \dfrac{vE}{1-v^2} - \dfrac{S_1S_2}{S} & \dfrac{E}{1-v^2} - \dfrac{S_1^2}{S} & -\dfrac{S_2S_6}{S} \\ -\dfrac{S_1S_6}{S} & -\dfrac{S_2S_6}{S} & \dfrac{E}{2(1+v)} - \dfrac{S_6^2}{S} \end{bmatrix}\begin{Bmatrix} d\varepsilon_x \\ d\varepsilon_y \\ d\gamma_{xy} \end{Bmatrix} = \left[D_p\right]\{d\varepsilon\} \tag{25}$$

And stress-strain equation

$$\sigma_{ij} = D_{ij}\varepsilon_{ij} \tag{26}$$

Used above equation authors can get the stress field.

3 PARTICLE MODELING

3.1 Title THREE DIMENSIONAL MODELING

To create computational models of the human head is placed polygon data in the boundary, or uses a three-dimensional voxel method to reconstruct CT/MRI medical images to partcile models. Here authors use CT/MRI medical images brightness to arrange for the initial particle coordinates by voxel method.

In the past, to reconstruct a three-dimensional model by CT/MRI medical images often used unstructured grid to reproduce the complex geometry, could not represent a solid model.

Authors use voxel data instead of polygon data. CT/MRI images are shot who ring-shaped by X-ray. Stacking height direction of ring-shaped slice images, make a three-dimensional model as figure2. Slice images is quantized by brightness value than corresponding to each head tissue. Using threshold selection by the brightness value as a scalar, extract three-dimensional volume data = voxel. Authors used medical image brightness to create particle models directly, so the modeling is easy to apply in SPH method.

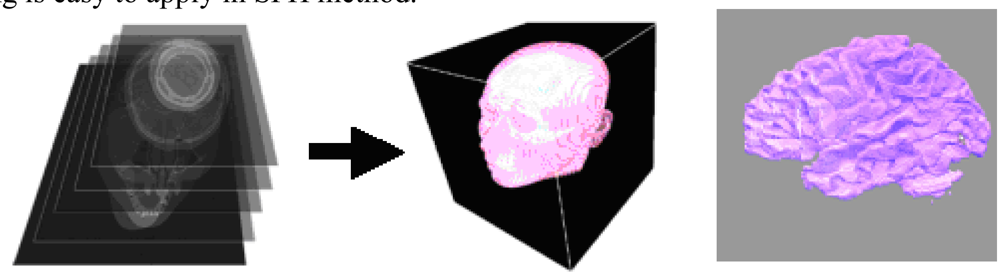

Figure2 three-dimensional model

But in general, high-resolution medical images are often used, so the data will be enlarged. Authors have to select a required resolution. This time, authors used the discrete frequency conversion of wavelet analysis method to be applied to medical images, and extending to three-dimension, to create a model for SPH analysis.

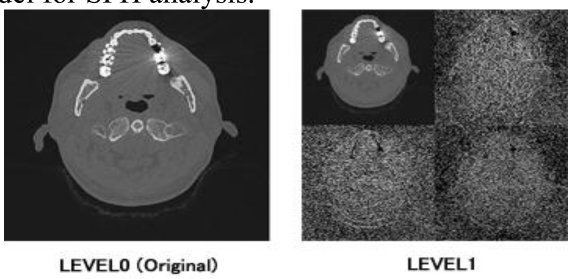

Figure3 Discrete wavelet transform to medical images

Used basic reference wave $\psi(t)$ and scaled or moved in parallel to fit the input signal, reference wave $\varphi_{j,k}(t)$ to transform.

$$\varphi_{j,k}(t) = 2^{-\frac{j}{2}}\varphi(2^{-j}t - k) \tag{29}$$

Here $\psi(t)$ used the simplest Haar Wavelet, the technique is like Figure 4. Authors reduced 512*512*512 resolution Three-dimensional images to any resolution images Figure 5. The compression trends will let original image to 1/512 Figure 6.

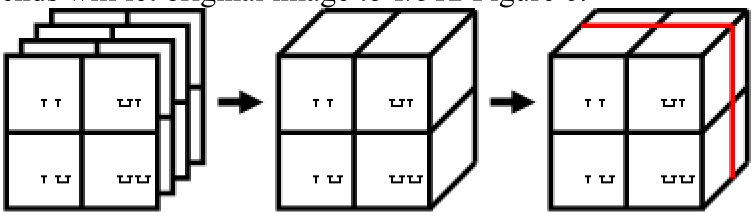

Figure4 3D Wavelet transform image.

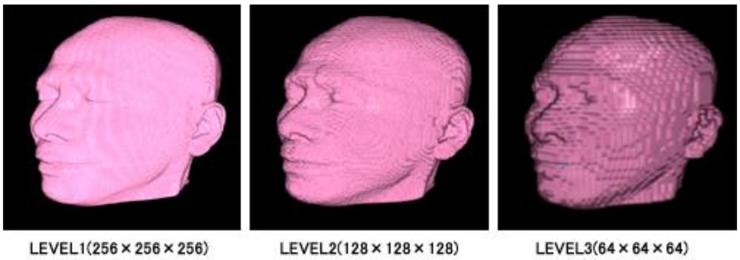

Figure5 Wavelet transform

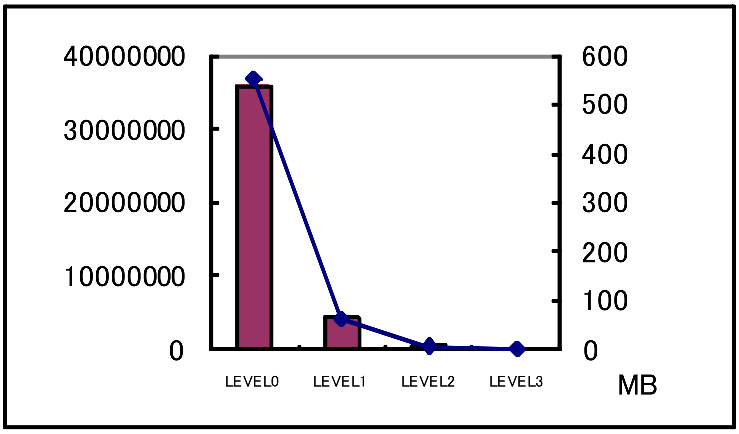

Figure6 the Wavelet transform compression trends

3.2 Real Time GPU Rending

Particle* volume data has a big problem that is data size too large. In this paper, authors used volume rendering on the GPU (Graphics Processing Unit), and can visualize experimental results in real time. Authors select two experimental methods. (1) Sampled texture on the GPU, the texture volume rending that can express property values based on the transfer function. (2) Sampled the particle data efficiently on GPU, ray casting in real time.

Texture rending is high affinity between GPU that easy to handle data of texture*color information. And also added rotation matrix to texture, always puts slice in the line of sight, to handle memory efficiently. Of course, polygons which map the particle data are used to cross each other with three-axis.

Ray casting is used in still image, it was not realistic to use in real time. Authors put volume on the GPU to take a sample, so ray casting allows real time processing. When the ray traverses the volume, if it beyonds the scope of ray or opacity exceeding its threshold, then terminates the calculation.

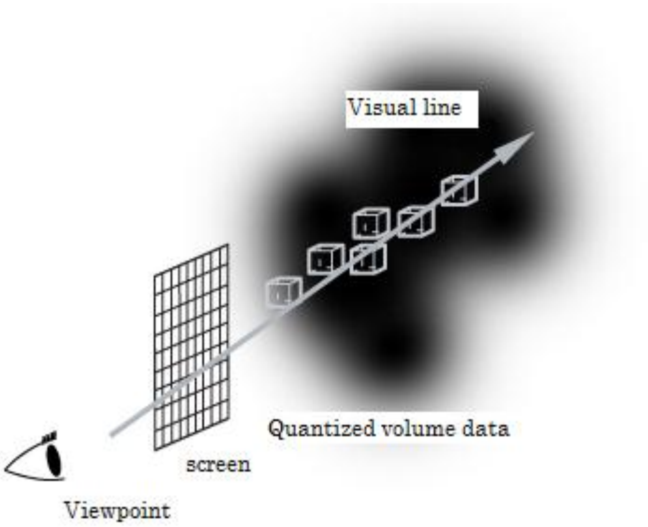

Figure7 Ray casting method image

This is a very useful technique for visualizing the internal state where in SPH visualizing.
Both of follow, throughput speed is 30～75FPS, Processing in real time is confirmed.

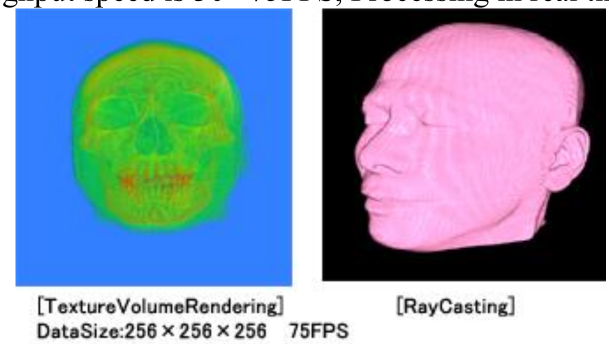

Figure8 GPU rendering

Apply Marching cubes method to isosurface maintain continuity, cell cube next to each other reverse, turn polygon over, obtained normal vector by cross product, and normal vector reverse easily too. So authors added Split tetrahedron method to avoid normal vector reverse.
Eq. (30) is determination of isosurface vertices.

$$\vec{r}_n = \frac{n_0 - n_j}{(n_i - n_j)}\left(\vec{r}_i - \vec{r}_j\right) \tag{30}$$

n : density of volume, n_0 :density range, i, j :grid r_n :isosurface vertices coordinates

$$\vec{\phi}_n = \frac{n_0 - n_j}{(n_i - n_j)}\vec{\phi}_i + \left(1 - \frac{n_0 - n_j}{(n_i - n_j)}\right)\vec{\phi} \tag{31}$$

ϕ : normal vector of attracting attention grid

As follow image is 1 slice 512*512 pixel, be 0.3mm thick, 386 pieces CT data by discrete wavelet transform and compress volume, 108 polygons.

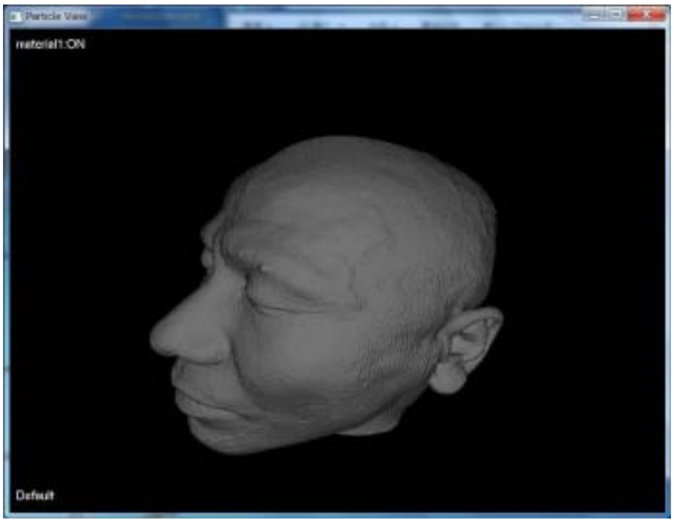

Figure9 accurate image

4 HEADINGS SPH ANALYSIS

As described modeling methods above, authors have been developed codes to make a human head computational model directly from CT/MRI images. The geometry of the model is based upon CT/MRI slices of a living human head and the particles represent an adult human head. Which has four parts: bones (include skin), brain, spinal fluid and meat tissue (include skin).

4.1 Analysis Condition

At first, authors made a simple model just had brain and bone.

Model : Brain:35 million particles,bone:15million particles

Impact condition: impact orientation : front, angle : 75° , impact speed : 30m/s

Image just like Figure10 .

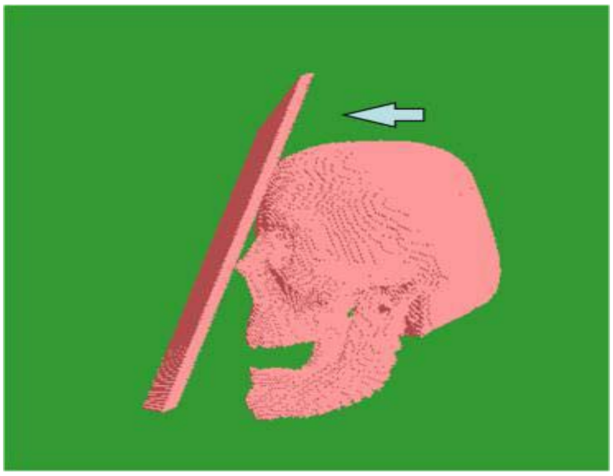

Figure10 Simulation model image

The second Model : Brain : 289793 particles, bone : 67122 particles, spinal fluid and brain fluid : 106706 particles, skin and meat tissue : 363854 particles

Impact condition : impact orientation : front, angle : 75° , impact speed : 30m/s

4.2 SPH simulation result

Figure11 is head impacted to wall and stress distribution

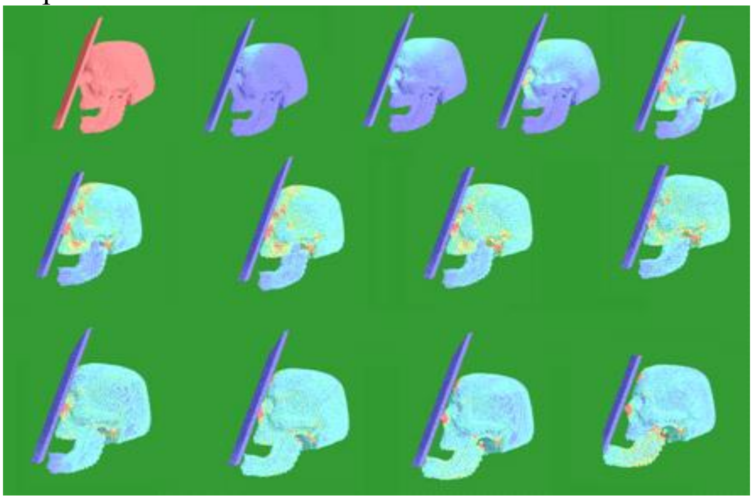

Figure11 Stress transmission from side view

Figure12 is brain pressure transmission.

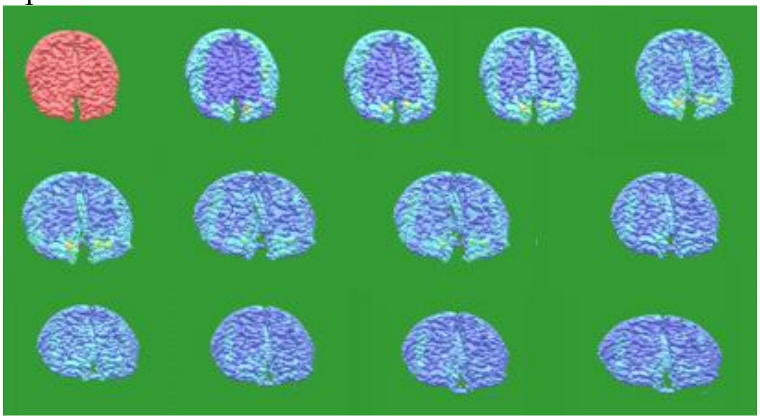

Figure12 brain pressure transmission

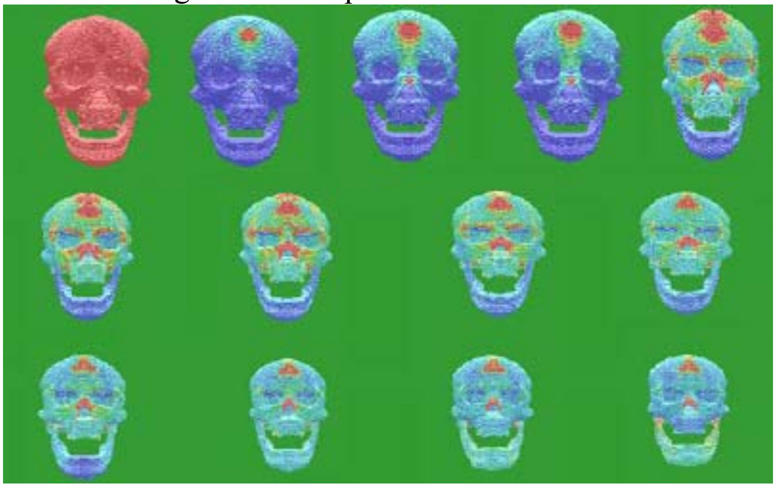

Figure13 Stress transmission from front view

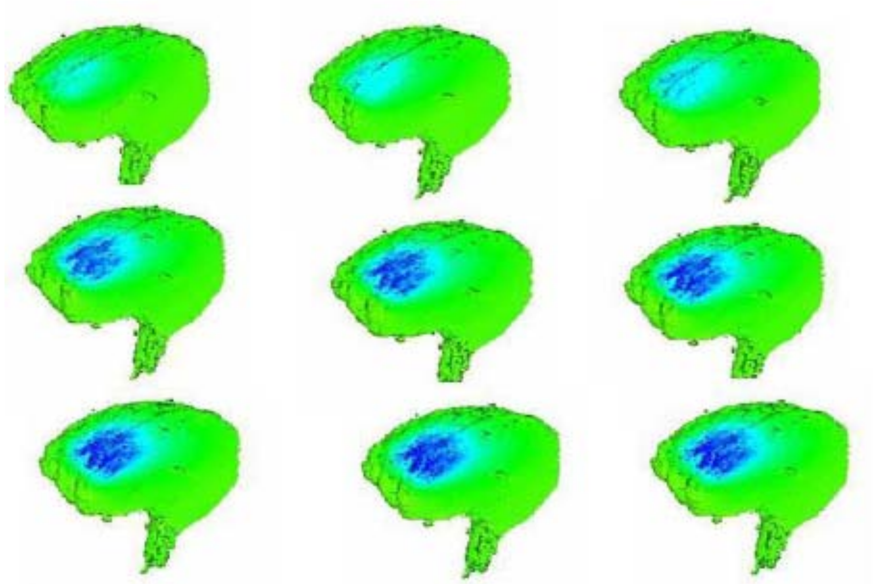

Figure14 precise model simulation result of brain pressure transmission

Stress is mises stress. Like the Figures showed collision parts had a large deformation and stress transmission clearly. Stress gradually is spread from outer to inside of brain. It has been observed high pressure occurs on the front of head when the impact from front or back. It is a match that is known, When traffic accident occurred, impacting from front to the head will be caused damage to the frontal region, impacting from back to the head will be caused damage to the front too.

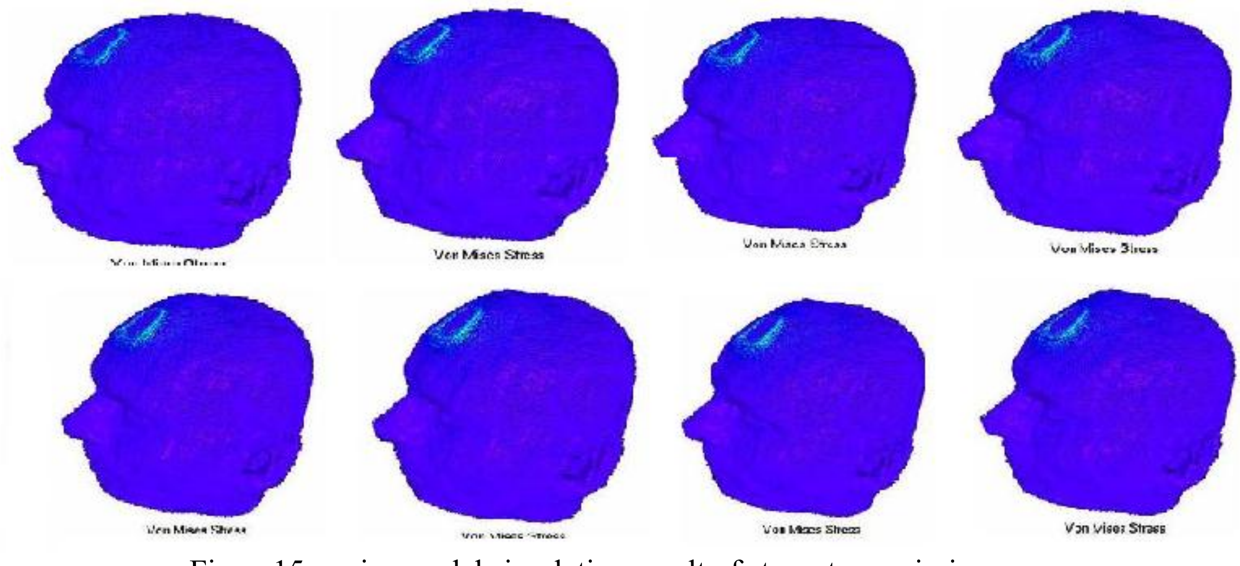

Figure15precise model simulation result of stress transmission

The simple model’s pressure is transferred from front to back, but precise model’s pressure is difficult to transfer from front to back, are expected.

The reason is the calculation added the brain fluid and spinal fluid which cushions, so pressure will be hard to transmission. And also need to change simulation conditions.

5 CONCLUSIONS

Authors addressed the problem of make a model from medical images directly, and simulate in high velocity impact of human head crash by SPH method. From now, authors need to make more precise human head model to assessment of human body injury (Include: fracture, retraction, amputate). And also authors must work for to apply SPH simulation and real time rending to three-dimensional virtual surgery (Include: dissection, ablation, bleeding).

Of course, in a traffic accident, head impact will come from any direction, authors need to calculate not only a head but also a man in the car or in other situation.

6 ACKNOWLEDGEMENT

Thank here, the CT/MRI was taken under the cooperation of teacher Tokyo Medical & Dental University Tsuruda Jun.

REFERENCES

[1] Lucy,L.B,,"a numerical approach to the testing of the fission hypothesis"Astron,J, 82,(1977),1013-1024

[2] Gingold,R.A,Monaghan,J.J.,"Smoothed particle hydrodynamics: theory and application to non-spherical stars",Monthly Notices of the Royal Astronomical Society 181(1977),375-389

[3] W.Benz, Smooth particle hydrodynamics: A review, Harvard-Smithsonian Center for Astrophysics, Preprint 2884,1989

[4] Monaghan,J.J.,Smoothed particle hydrodynamics, Annu Rev. astron. Astrophys. 30(1992) 543-574

[5] L.D. Libersky and A.G. Petschek, Smooth particle hydrodynamics with strength of materials, Advances in the free Lagrange Metho , Lecture Notes in Physics 395(1990) 248-257

[6] Johnson., G. R, A.G. Petscheck and R.A. Stryk, Incorporation of an SPH option in the EPIC code for a wide range of high velocity impact computations, Int.J. Impact Engrg. 14 (1993) 385-394

[7] A.G. Petschek and L.D Libersky, Cylindrical smoothed particle hydrodynamics, J. Cmput.Phys. 109 76-83 (1993)

[8] Swegle, J.W., Attaway, S.W., Heinstein, M.W., Mello, M.W., Hicks, D.L., "An Analysis of Smoothed Particle Hydrodynamics", Report No. SAND93-2513-UC-705, Sandia National Laboratory, Albuquerque, NM, (1994).

[9] S. Koshizuka, H. Tamako and Y. Oka , A Particle Method for Incompressible Viscous Flow with fluid Fragmentation, *Computational Fluid Dynamics Jounal*, 4, 1, (1995),pp.29-46.

[10] Johnson., G. R., "Artificial viscosity effects for SPH impact computations", International Journal of Impact Engineering, Volume 18, Number 5, July 1996, pp. 477-488.

[11] Nick Foster and Dimitri Metaxas. Realistic animation of liquids. *Graph.Models Image Process.*, Vol. 58, No. 5, pp. 471–483, 1996.

[12] Song moo seop, Sakai Yuzuru,Yamasita Akihiko "Elastic-plastic Analysis by SPH method:1st report,Small displacement problem in 2-Dim " JSME,A 68(669) pp.772-778(20020525)

[13] Sakai Yuzuru, Yang zongyi, Jung youngguan,Imcompressible viscous flow analysis by SPH,JSME,B70,666,(2004-8)

[14] Tanaka, Analysis of flow between Red Cell and Fluid with MPS method, The 18th CFD symposium C2-3(2004)

[15] Mark Carlson, Peter J. Mucha, and Greg Turk. Rigid fluid: animating the interplay between rigid bodies and fluid. *ACM Trans. Graph.*, Vol. 23, No. 3, pp. 377–384, 2004.

[16] KoukPoh Tang, Yuzuru Sakai, Nobuki Yamagata: Heat conduction and Heat convection Analysis by SPH Method, JSME 18th Computational Mechanics Conference [No.05-2] pp.585-586,(2005)

[17] Y. Zhu and R. Bridson: Animating Sand as a Fluid, SIGGRAPH'05, pp. 965-972 (2005)

[18] Jos Stam. Stable fluids. In *Proceedings of the 26th annual conference on Computer graphics and interactive techniques*, pp. 121–128. ACM Press/Addison-Wesley Publishing Co., 1999.

[19] Oh-Young Song, Hyuncheol Shin, and Hyeong-Seok Ko. Stable but nondissipative water. *ACM Trans. Graph.*, Vol. 24, No. 1, pp. 81–97, 2005.

[20] Zanuttigh, B., Lamberti, A.: Experimental analysis of the impact of dry avalanches on structures and consequences for debrisflows. J. Hydraul. Res. 44(4), 522–534 (2006)

[21] Chin G L, Lam K Y, Liu G R. *Advances in Meshfree and X-FEM Methods* [M]. Liu G R Ed. World Scientific, Singapore , 2002.

[22] Johnson., G. R. and S.R Beissel, Normalized smoothing functions for SPH impact computations, Int. J. Numer . Methods Engrg., Accepted for publication

[23] S.W Attaway, M.W. Heinstein and J.W. Swegle, Coupling of smooth particle hydrodynamics with the finite element method, Nucl. Engrg. De. 150 199-205 (1994)